

YMTHE, Volume 25

Supplemental Information

Direct Head-to-Head Evaluation of Recombinant Adeno-associated Viral Vectors Manufactured in Human versus Insect Cells

Oleksandr Kondratov, Damien Marsic, Sean M. Crosson, Hector R. Mendez-Gomez, Oleksandr Moskalenko, Mario Mietzsch, Regine Heilbronn, Jonathan R. Allison, Kari B. Green, Mavis Agbandje-McKenna, and Sergei Zolotukhin

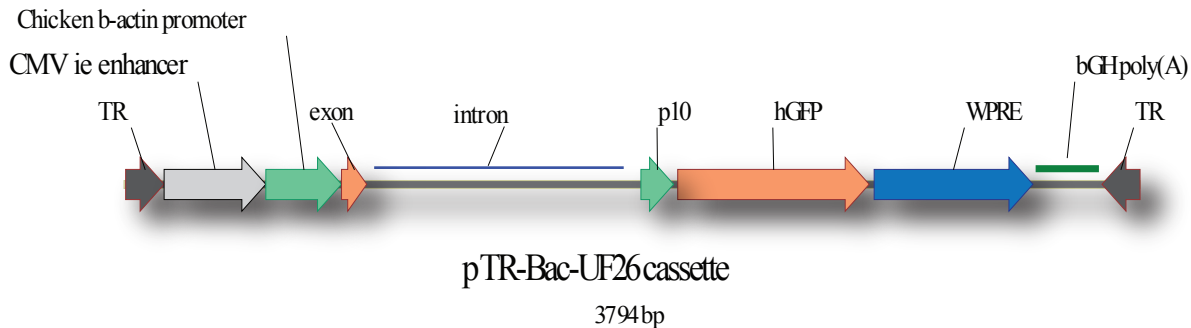
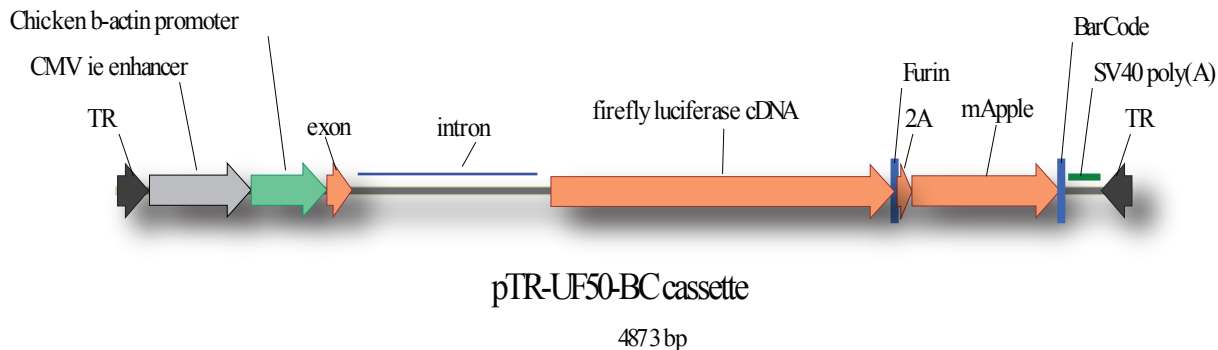
A**B**

Figure S1. Annotated graphical maps of rAAV cassettes packaged into rAAV5 and rAAV9 capsids.
 (A) pTR-Bac-UF26 cassette. (B) pTR-UF50-BC cassette (to Fig. 4).

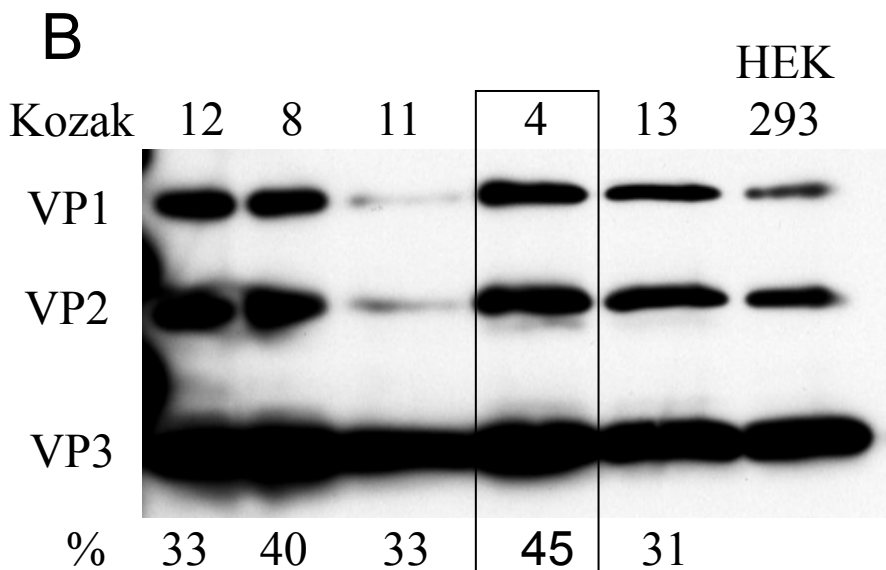
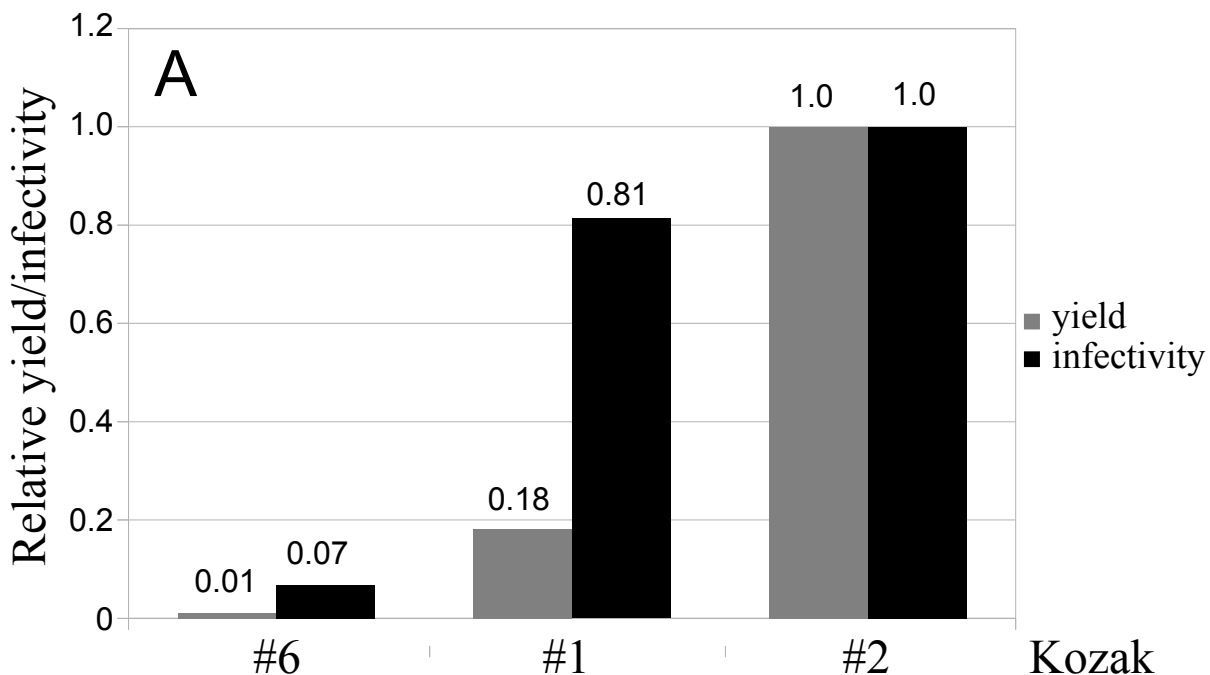


Figure S2. Characterization of infectivity and capsid composition of selected capsid helper constructs.

A – Relative yield-to-infectivity ratios of purified rAAV5 produced in Sf9 stable cell lines incorporating Kozak sequences 6, 1, and 2 (to Fig. 1, Table S1).

The selected Kozak 2 produced the highest relative yield-to-infectivity ratio.

B – Capsid composition of purified rAAV9 produced in Sf9 stable cell lines incorporating Kozak sequences (Table S1).

The identical amounts of purified viral particles (10×10^{11} vg) were loaded in each lane. The selected Kozak 4 (boxed) produced the highest infectivity in vitro among tested.

HEK 293

VP1

*

VP2

VP3

Sf9 B8

VP1

VP2

VP3

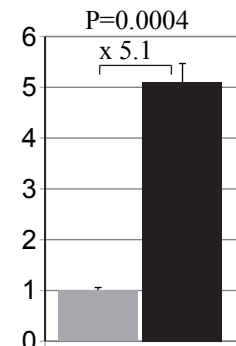
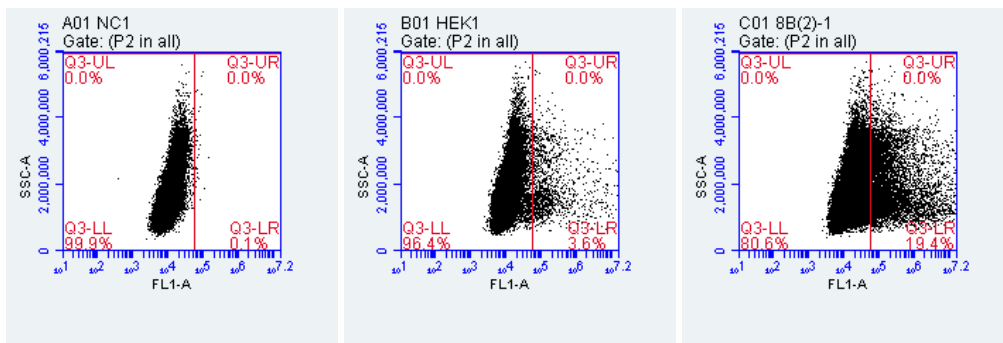
Figure S3. Scanned profiles of rAAV5 preparations separated by SDS-PAAG electrophoresis.

Shaded areas indicate areas-under-the-curves (AUCs) outlined for quantifications.

(*) indicates the peak excluded from the analysis (to Fig. 1 and 2).

A

rAAV5



B

rAAV9

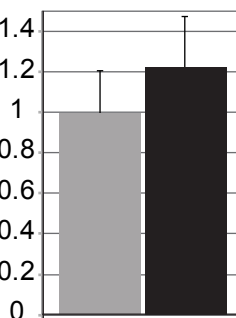
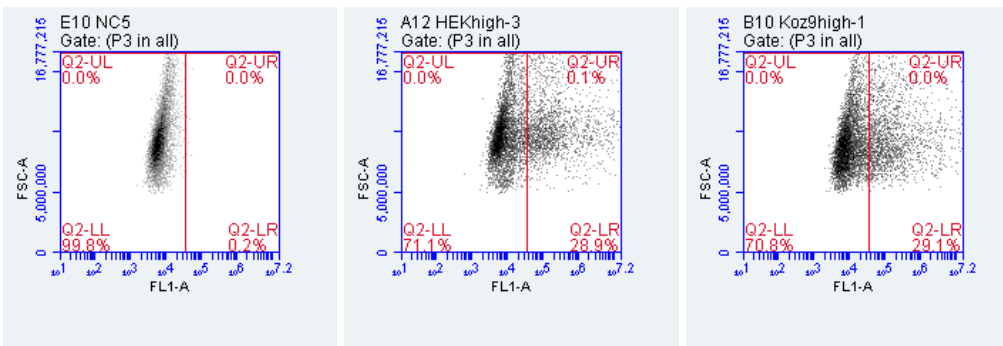


Figure S4. In vitro transduction assay of rAAV-UF50-BC packaged into rAAV5 or rAAV9 capsids.

A. Fluorescence-activated cell sorting (FACS) and its graphic quantification of rAAV5-UF50-BC.

B. Fluorescence-activated cell sorting (FACS) and its graphic quantification of rAAV9-UF50-BC

(to Fig. 4).

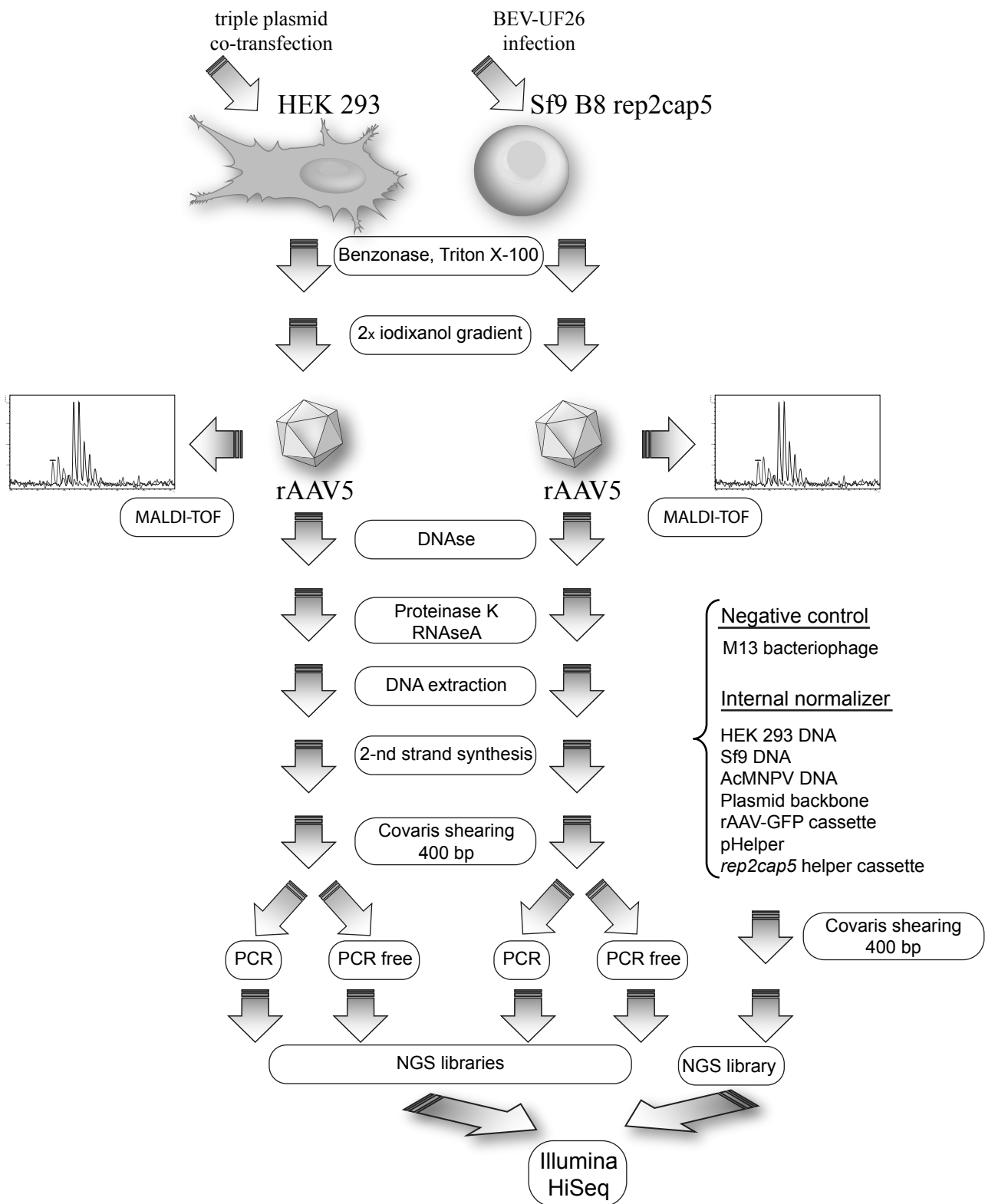


Figure S5. Schematic flowchart of rAAV5 vector DNA preparation for NGS.

All steps for HEK 293-derived and Sf9-derived rAAV5 vectors were performed side-by-side (to Table 1).

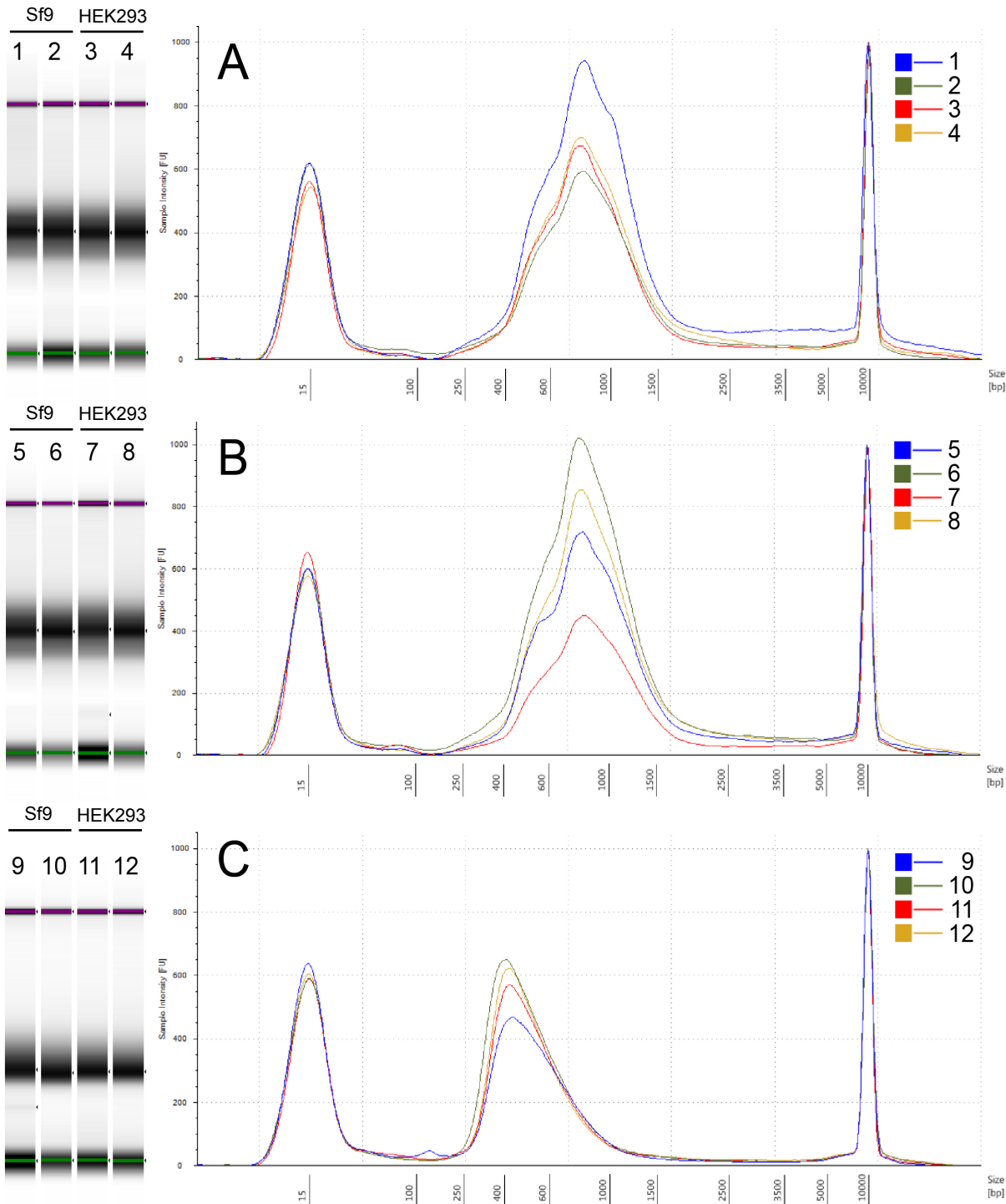


Figure S6. Distribution of NGS libraries DNA fragment sizes. Analysis of synthesized NGS libraries by High Sensitive D5000 ScreenTape: A. PCR-free libraries sequenced directly by NGS: 1,2 - rAAV5/Sf9; 3,4 - rAAV5/HEK 293; B. PCR-free libraries used for low cycle PCR enrichment: 5,6 - rAAV5/Sf9, 7,8 - rAAV5/HEK293; C - PCR-enriched libraries: 9, 10 - rAAV5/Sf9; 11, 12 - rAAV5/HEK 293. Libraries 9-12 were sequenced directly by NGS (to Table 1).

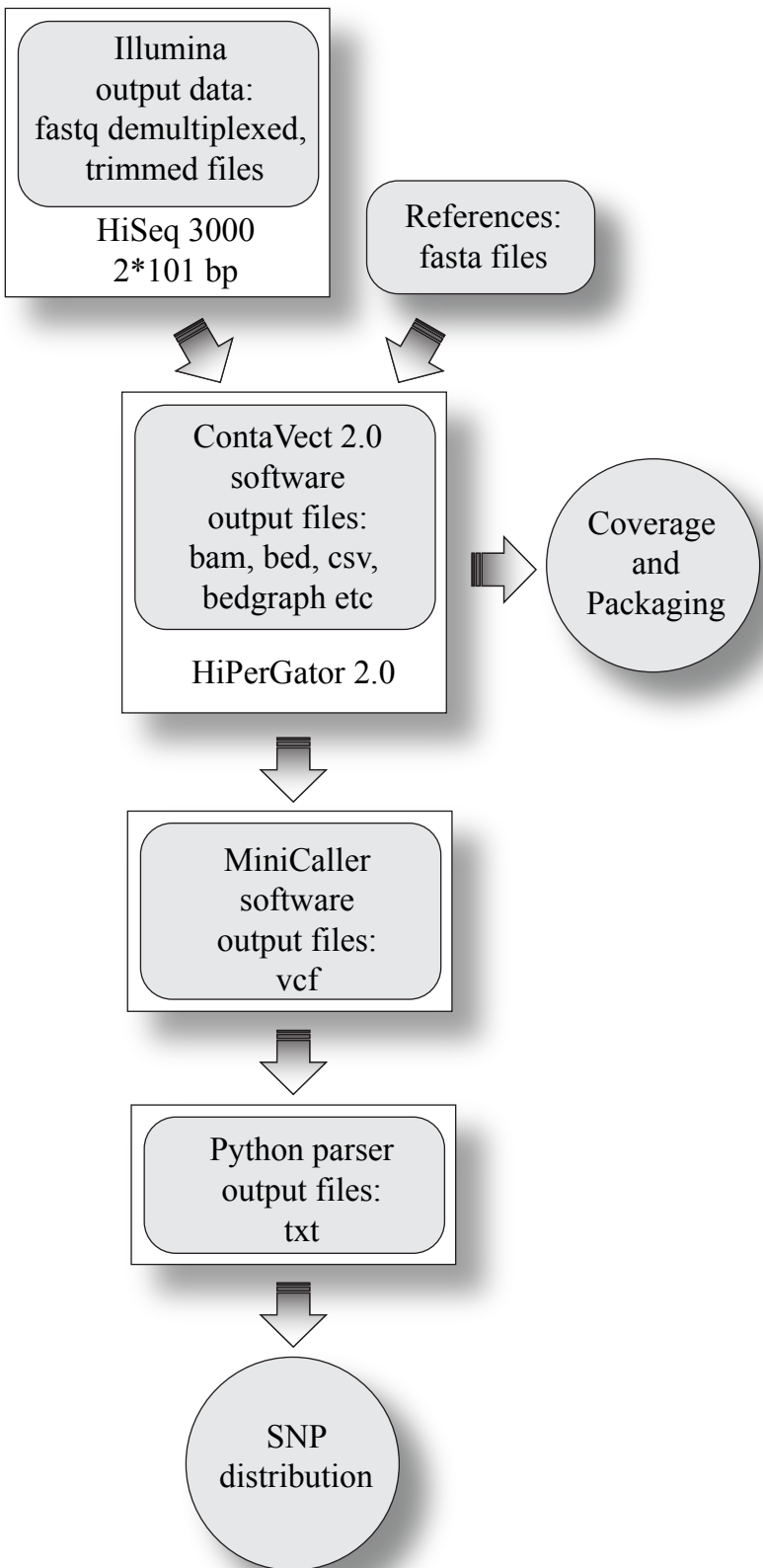


Figure S7. Schematic flowchart of NGS data processing.

All calculations were performed on the UF Research Computing HiPerGator supercomputer (to Table 1).

Table S1. WT and attenuated TISs tested for the expression of AAV5 and AAV9 capsid genes (to Fig. 1).

	Sequence	Efficiency (%)*
AAV5 Koz VP1		
wtAAV5	GUAGUCA <u>AUGUC</u>	91
1	UCUUUU <u>AUGUC</u>	43
2	UGUUUU<u>AUGUC</u>	40
3	UAGUUU <u>AUGUC</u>	37
4	UAGUGU <u>AUGUC</u>	33
5	CAUUGU <u>AUGUC</u>	32
6	UCGUUU <u>AUGGA</u>	30
7	CAGUUU <u>AUGGU</u>	20
8	CAUUGU <u>AUGGU</u>	16
9	UAGUGU <u>AUGCU</u>	14
10	CAUUGU <u>AUGCU</u>	12
AAV9 Koz VP1		
wtAAV9	CCAGGU <u>AUGGC</u>	130
1	UCUUUU <u>AUGGC</u>	57
2	UGUUUU <u>AUGGC</u>	54
3	UAGUUU <u>AUGGC</u>	50
4	UAGUGU<u>AUGGC</u>	45
5	UCUUUU <u>AUGGG</u>	43
6	UCUUUU <u>AUGUC</u>	43
7	UGUUUU <u>AUGGG</u>	42
8	UGUUUU <u>AUGUC</u>	40
9	UAGUUU <u>AUGGG</u>	38
10	UAGUUU <u>AUGUC</u>	37
11	UAGUGU <u>AUGGG</u>	33
12	UAGUGU <u>AUGUC</u>	33

*Estimated relative TIS efficiencies¹⁸.

Selected sequences for each serotype are highlighted in bold. Underline indicates the VP1 start codon.

Table S2. VP1/VP3 ions, intensities and ratios (to Fig. 2).

Ion, M/Z*	HEK, VP1/VP3				B8, VP1/VP3			
	I	II	III	Average	I	II	III	Average
1464	0.029	0.031	0.022	0.027	0.101	0.13446	0.101408	0.11228932
1677	0.057	0.059	0.018	0.045	0.1123019	0.1475244	0.123	0.12760876
2051	0.04	0.038	0.026	0.035	0.178	0.1548061	0.09411	0.14230537
Total Average: 0.036				Total Average: 0.127				

* M/Z represents mass divided by charge number.

Table S3. VP2/VP3 ions, intensities and ratios (to Fig. 2).

Ion, M/Z*	HEK, VP2/VP3				B8, VP2/VP3			
	I	II	III	Average	I	II	III	Average
1464	0.046521	0.045163	0.037953	0.043	0.177247	0.203963	0.218152	0.1997873
1677	0.045479	0.044517	0.027105	0.039	0.162602	0.178148	0.150699	0.1638163
2051	0.040742	0.031026	0.031464	0.034	0.22123	0.137658	0.165207	0.1746982
Total Average: 0.039				Total Average: 0.179				

* M/Z represents mass divided by charge number.

Table S4. Total number of Illumina reads analyzed for rAAV5 produced in HEK 293 cells (to Table 1).

Sequence reference	Number of reads			
	PCR-free*		PCR-enriched*	
UF26 cassette	82262561	60130733	37549520	40902323
Backbone	2195873	1571017	1376960	1454155
pHelper	34612	23137	16865	17829
<i>rep/cap</i>	601194	425165	393207	415390
Genomic DNA	149013	103661	88603	93199
Unmapped_and LowMapq	2916120	2085563	590382	640031

* Each referenced sample was prepared, sequenced, and analyzed in duplicates.

Table S5. Total number of Illumina reads analyzed for rAAV5 produced in Sf9 cells (to Table 1).

Sequence reference	Number of reads			
	PCR-free*		PCR-enriched*	
UF26 cassette	92293074	50662242	42762178	37098393
Backbone	274542	151788	178719	154424
<i>rep/cap</i>	12983	7518	1192	1081
Baculovirus/Bacmide	268990	137477	170322	127495
Genomic DNA	23574	12677	12677	15129
Unmapped and LowMapq	1264002	688674	446306	346939

* Each referenced sample was prepared, sequenced, and analyzed in duplicates.

Supplemental Video 1. Representative video of visualized gold-labeled AAV particles.
For each sample, 30 seconds video was recorded 3 times (to Fig. 3).